THE JOURNAL OF PHYSICAL CHEMISTRY B

Article

pubs.acs.org/JPCB

Predicting the Coordination Number within Copper Chaperones: Atox1 as Case Study

Tamar Ansbacher[†] and Avital Shurki*[,†,‡]

[†]Institute for Drug Research, School of Pharmacy, Faculty of Medicine, The Lise-Meitner Minerva Center for Computational Quantum Chemistry, The Hebrew University of Jerusalem, Jerusalem 91120, Israel

Supporting Information

ABSTRACT: The concentration of copper ions in biological systems is tightly regulated by metallochaperone proteins which are responsible for Cu(I) delivery to designated locations in the cell. These proteins contain a unique motif (MXCXXC) that binds Cu(I) very tightly and specifically but at the same time allows efficient metal transfer to target proteins that often contain a similar copper binding motif. It was found that binding to Cu(I) is achieved through the two cysteine residues in a low coordination number of 2−3 due to possible binding of a third external ligand. Understanding copper transport requires better understanding of copper coordination. Here we therefore focused on establishing a computational method that can predict the coordination number of copper in copper chaperones. The method is shown to be successful in predicting the coordination of Cu(I) within the human copper chaperone (Atox1). Based on the results, a possible rationale for this unique Cu(I) dicoordination in Atox1 is suggested.

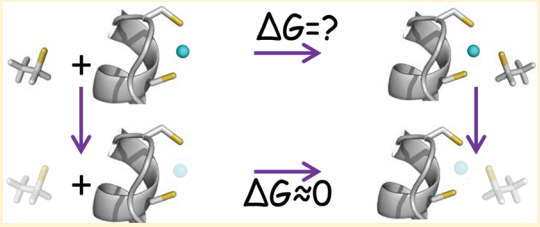

INTRODUCTION

Copper is a late transition metal that serves as a cofactor in several essential biological processes due to its ability to cycle between two oxidation states, Cu(I) and Cu(II). The free form of Cu(I) is highly reactive and may cause oxidation damage. As a result, the concentration of copper in the cell is tightly regulated by copper binding proteins called copper chaperones.[1−3] These proteins bind copper tight and deliver it to various target proteins in the cell, while preventing undesired chemistry to occur.[4] Breakdown in copper trafficking and access or deficiency of copper ions are hence associated with a variety of neurodegenerative diseases such as Alzheimer's disease,[5,6] Parkinson's disease, ALS,[7] Menkes syndrome, and Wilson disease.[8,9]

Atox1 (also referred to as Hah1) is a cytosolic human copper chaperone that serves as a key protein in Cu(I) homeostasis. Atox1 binds and delivers Cu(I) ions to two P-type ATPases that couple ATP hydrolysis with Cu transport across membranes: the Wilson and Menkes disease proteins. Understanding the molecular details of Cu(I) binding coordination and transport pathways is, therefore, crucial for studying these human diseases.[10,11]

Both the crystal structure and the solution structures of Cu(I)-bound Atox1 revealed a ferredoxin-like fold with a $\beta\alpha\beta\beta\alpha\beta$ structure, in agreement with all other copper chaperones.[12−14] Furthermore, the highly conserved motif $MX_1CX_2X_3C$ (M is methionine, X_1 is usually threonine or serine in eukaryotic and prokaryotic copper chaperones, respectively, C is cysteine and X_2, X_3 are any amino acid), which is situated in all other copper chaperones on a flexible solvent-exposed loop at the beginning of the first α helix, was found for Atox1 as well.[14] Yet, with regards to the coordination of Cu(I), it seems that the patterns that govern Atox1 are somewhat different from those of the other copper chaperones.

The solution structure of holo-Atox1, which involves a monomer, exhibits a dicoordinated Cu(I) center where Cu(I) is bound to the two conserved cysteines.[14] Similarly, EXAFS studies of Atox1 support a linear two-coordinated Cu(I) center.[15] These findings are fairly surprising given that dicoordinated Cu(I) in small organic complexes involving sulfur atoms is quite rare and usually either tetra- or tricoordination is observed.

The crystal structure of Atox1 bound to Cu(I) involves a dimer with Cu(I) in a distorted tetrahedral environment bound to three cysteine residues and a fourth cysteine involved in a secondary interaction.[12] This structure suggests tri- or (though less likely) even tetracoordination for copper. Yet, it is believed to represent a transient complex which is formed upon copper transfer from Atox1 to the target protein,[3,12] as was recently suggested by various studies of the interactions between Atox1 or its respective homologues and the relevant target proteins.[16−20]

In both yeast and bacteria homologues of human Atox1, Cu(I) is generally suggested to be tricoordinated.[21−23] Particularly, the solution structure of Cu(I)-bound Atx1 (the yeast homologue of Atox1) suggested a trigonal environment, involving two cysteines and a third unidentified ligand.[21,24] EXAFS data classified the identity of the third ligand as a thiol, thus supporting a tricoordinated structure.[24] On the other hand, while Cu(I)-bound Atx1 has not yet been crystallized,

Received: November 7, 2011
Revised: February 11, 2012
Published: April 5, 2012

   dx.doi.org/10.1021/jp210678n | J. Phys. Chem. B 2012, 116, 4425−4432

Hg(II)-bound Atx1 exhibited dicoordination.[25] Similarly, the solution structure of Cu(I)-bound CopZ (the bacteria homologue of Atox1) demonstrated a S−Cu−S angle of 115° ± 26°, indicating involvement of an exogenous third ligand, a suggestion which was supported also by EXAFS studies.[22,23] Yet, the crystal structure of CopZ dimer demonstrated tetranuclear Cu(I) clusters. Here two subsets of Cu(I) ions were identified: two outer Cu(I) ions that exhibit distorted trigonal coordination and two inner Cu(I) ions that exhibited distorted digonal coordination.[26]

The above findings indicate that understanding copper transport in the cell requires better understanding of copper coordination. It is therefore useful to establish a theoretical method that can predict the coordination number of copper in copper chaperones.

Few theoretical studies have tried to validate the experimentally observed coordination number in several different copper chaperones. Dalosto investigated the copper binding site of Atx1 using quantum mechanics/molecular mechanics (QM/MM) methods and found the Cys(S)−Cu−Cys(S) angle to be 166°,[27] compared to 120 ± 40° which was reported experimentally.[21] He concluded that Atx1 is coordinated to two sulfur atoms in a nearly linear arrangement. His calculations found a very shallow potential energy surface for the Cys(S)−Cu−Cys(S) bending mode. He thus used this finding to explain the source of disorder detected in the crystallographic and NMR studies.[27] Rodriguez-Granillo and Wittung-Stafshede studied the Cu-binding geometry of Atox1 and CopZ (*Bacillus subtilis* homologue of Atox1) using QM/MM. Their optimized geometries for the holo-proteins suggested that Cu(I) favors a linear Cys(S)−Cu−Cys(S) arrangement in Atox1 in agreement with experiment. CopZ exhibited a calculated angle which is close to 150°,[28] compared with the EXAFS and NMR estimations of 115 ± 26°.[22,23] They concluded that CopZ involves a distorted linear Cu(I) coordination, which is imposed by the protein structure, rather than a trigonal coordination as suggested by experiments. This conclusion is based on the fact that bent geometry was a result of the optimization in the absence of a third ligand.[28] They also tested whether the conserved Met11 is capable of binding Cu(I) and showed that in its absence no major geometrical changes take place, suggesting that Met11 is not a Cu(I) ligand.[28] None of these studies, however, calculated the relative energies of the various possible coordination states of Cu(I) in the binding site.

Holt and Merz have compared calculated coordination of two, three, and four both in vacuum and in aqueous solution using a small model of the Cu(I) binding site from Atox1 where methylthiolate (CH_3S^-) and methylthiol (CH_3SH) served as the ligating and nonligating cysteine residues, respectively. The four-coordinate state was found to be energetically unfavorable while the two-coordinate state was suggested to be the most stable both in vacuum and in aqueous solvent.[20] They concluded that a four-coordinate intermediate in the Cu(I) transport mechanism between Atox1 and the fourth metal binding domain (MBD) of the Menkes disease protein (MNK4) is not likely to exist. Regarding two- or three-coordination of Cu(I) in the Cu(I) transfer, they did not make any conclusions, as their calculations predicted a large energetic penalty which they considered as exaggerated. They stated that the calculations did not take into account the effect of the protein environment that can in principle play a major role.[20]

Finally, Wittung-Stafshede and co-workers used QM/MM methods to shed light on the reaction mechanism of Cu(I) transfer from Atox1 to the fourth MBD of Wilson disease protein (WD4). All possible two-, three-, and four-coordinate Cu(I)-intermediate species in the Atox1−WD4 complex were assessed geometrically and energetically, and one dominant reaction path was proposed.[19] The Cu-transfer reaction from Atox1 to WD4 was found to be kinetically accessible but endothermic, in contrast to recent experimental findings,[29] and the authors pointed a finger at the entropic effects that were not taken into account in the calculations.[19]

Based on these studies, proper prediction of the coordination number seems to be a rather challenging task. In this work we propose a quantitative tool for proper prediction of the coordination number of metals in a protein environment and in particular Cu(I) in copper chaperones. Recently, we established a reliable level of calculation for prediction of coordination number in small Cu(I) complexes with aromatic thiolato ligands.[30] Here we first examine the performance of the method on small, experimentally known,[31] Cu(I) complexes with aliphatic thiolato ligands, which resemble better cysteine residues as ligands. We then utilize a thermodynamic cycle to calculate the reaction free energy for the association of a third external thiolato ligand to a dicoordinated Cu(I) in Atox1. Our method is shown to be able to quantitatively predict the correct coordination number of copper within the Atox1 protein environment. Based on the results, a rationale is given to the special dicoordination of Cu(I) within Atox1.

METHODOLOGY

The key objective is to be able to discriminate energetically between di- and tricoordinated Cu(I) within the protein. The natural way to do so is to assess the reaction energy, ΔE_0, for the following association reaction:

$$CuL_2^{-1} + L^{-1} \rightarrow CuL_3^{-2} \quad (1)$$

where L represents any ligand and ΔE_0 is defined by eq 2. A preference for a tricoordinated Cu(I) complex should result in a negative reaction energy ($\Delta E_0 < 0$), whereas preference for a dicoordinated Cu(I) complex should result in a positive reaction energy ($\Delta E_0 > 0$):

$$\Delta E_0 = E(ML_3^{-2}) - [E(ML_2^{-1}) + E(L^{-1})] \quad (2)$$

This method, however, while sufficient and useful for the prediction of Cu(I) coordination of small Cu(I) complexes (e.g., ref 30) cannot be used in a straightforward manner to predict the coordination number in a protein environment, due to the large conformational space, and here reaction free energy should be addressed. We have, therefore, utilized two distinct thermodynamic cycles to assess the reaction free energy. One cycle (Scheme 1), referred to as the multiple step cycle, involved first calculating the solvation free energy of the third-external thiolato ligand in both the di- and tricoordinated states. That is, calculating the interaction of that ligand with the remaining system. This was done by calculating the reaction free energy for setting the partial charges of each of the ligand's atoms to zero ($\Delta G_{a\rightarrow b}$ and $\Delta G_{e\rightarrow d}$, respectively, in Scheme 1). Then the solvation free energy of copper was calculated also, both in the di- and tricoordinated states. This was done by now evaluating the free energy for setting copper's charge to zero ($\Delta G_{b\rightarrow c}$ and $\Delta G_{f\rightarrow e}$, respectively, in Scheme 1). Further details clarifying the nature of the calculated hypothetical reactions and

dx.doi.org/10.1021/jp210678n | J. Phys. Chem. B 2012, 116, 4425−4432

Scheme 1. The Two Thermodynamic Cycles Used To Calculate the Reaction Free Energy[a]

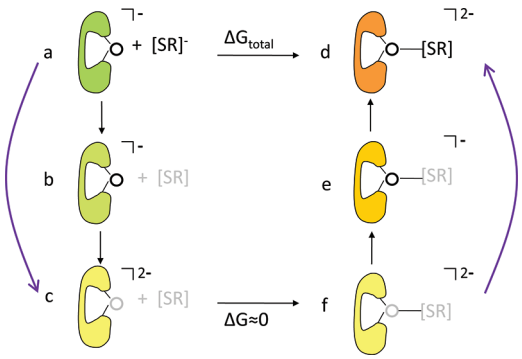

[a]The multistep cycle is presented by the full depicted cycle, whereas the two-step cycle is depicted by the cycle defined by the round purple arrows. Fragments whose charges are set to zero are colored gray. Different colors of the proteins present the different protein configurations which are adjusted to the charge distribution.

the respective ΔG's are given in Supporting Information (Schemes S1 and S2).

The second cycle, referred to as the two-step cycle, involved calculating the solvation free energy of both copper and the third thiolato ligand simultaneously in both the di- and tricoordinated states. This was done by simultaneously setting their partial charges to zero ($\Delta G_{a\rightarrow c}$ and $\Delta G_{f\rightarrow d}$, respectively, in Scheme 1). Further details can be found in Supporting Information (Schemes S1 and S2).

In both cycles, the reaction free energy for the last (hypothetical) step ($\Delta G_{c\rightarrow f}$) can be approximated as zero. Neither copper nor the external ligand are charged in that step, and the charge distribution of the remaining two Cys residues is identical (Φ_3 and Φ_3' in Scheme S1 of Supporting Information). As a result, the protein configuration-distribution is not expected to differ much between the two states, and the energy differences (both electrostatic and van der Waals) are therefore likely to be negligible.

Using these thermodynamic cycles, the free energy for the association of an external ligand to a dicoordinated Cu(I) in the protein is described by eqs 3 and 4 for the multiple-step and two-step cycles, respectively.

$$\Delta G_{a\rightarrow d} = \Delta G_{a\rightarrow b} + \Delta G_{b\rightarrow c} + \Delta G_{f\rightarrow e} + \Delta G_{e\rightarrow d} \quad (3)$$

$$\Delta G_{a\rightarrow d} = \Delta G_{a\rightarrow c} + \Delta G_{f\rightarrow d} \quad (4)$$

COMPUTATIONAL DETAILS

QM Calculations. *Geometries.* All geometries were optimized at the B3LYP level using the 6-31G* basis set, which was shown in previous studies to yield relatively good geometries (e.g., refs 30, 32−34). Optimizations were carried out in the presence of aqueous solvent corrections simulated by means of the polarizable continuum model (IEF-PCM).[35] For the small Cu(I) complexes, optimizations were carried out in a simulated THF solvent as well, because that was their crystallization solvent. Furthermore, geometries of these complexes were all characterized by frequency analysis to ascertain that these are indeed local minima (optimized geometries in both solvents can be found in Tables S1−S4 of Supporting Information).

Single Point Energies. Once geometries were available, single-point energy calculations were carried out at the PBE0 level.[36,37] We used the Pulay's modified m6-31G* basis set for Cu,[38] combined with the 6-31+G* basis set on the remaining elements[39] (referred to as m6-31+G* hereafter). Zero-point vibrational energies (ZPVE) were calculated at the respective optimization level, unless otherwise stated. Basis set superposition error (BSSE) was calculated at the single point level (i.e., PBE0/m6-31+G*) using the Boys−Bernardi counterpoise approach.[40] Finally, van der Waals (VdW) interactions, which are known to be inadequately covered by conventional DFT approaches, were considered by using Grimme's dispersion correction,[41,42] with a global scaling factor s_6 = 0.7, which was obtained for the PBE0 functional.[43] This PBE0/m6-31+G* level of calculation with the ZPVE, BSSE, and VdW corrections was shown to be useful for prediction of the coordination number of Cu(I) complexes.[30] All the quantum calculations reported in this work were performed with the Gaussian 09 package.[44]

QM/MM Calculations. *Starting Geometries.* The starting coordinates for Atox1 are based on solution structures of holo-Atox1 taken from the 1TL4 code in the Brookhaven Protein Data Bank (PDB).[14] Three out of an ensemble of thirty NMR models: the second, sixth, and eighteenth in the PDB (referred to as 1TL4.2, 1TL4.6, and 1TL4.18 hereafter), known to have a coordination of two, were selected for the calculations. All these structures consist of copper bound via two cysteine residues. Thus, in order to model the tricoordinated species a third-external cysteine-like ligand was added to the starting geometry. Cu(I) and the three cysteine ligands define the reactive-quantum region, while the rest of the protein with the explicit water molecules define the MM region. The three cysteine ligands were considered only in their ionized form and modeled in the quantum calculations by ethylthiolate ($CH_3CH_2S^-$), following the recommendation of Rosch and coworkers.[45] In some cases the side chain of the conserved Lys (Lys60), was also included in the reactive-quantum region (modeled as $CH_3CH_2CH_2CH_2CH_3NH_3^+$).

The position of Cu(I) in the NMR structures, originally obtained by MM calculations, is based on the position of the protein residues and, in particular, the cysteine sulfur atoms.[14] Its position, therefore, largely depends on both the force field (FF) utilized and the quality of the configurational sampling. Furthermore, the initial position of the external ligand, which is not part of the solution structure, is arbitrary and was chosen by us to be 12.0 Å and 2.3 Å from Cu(I) in the di- and tricoordination structures, respectively. Therefore, the position of both Cu(I) and the external ligand were refined in the protein frame using two different optimization procedures. The first involved only the quantum part atoms (including Cu(I) and three cysteine-like molecules) optimized in aqueous solution modeled by PCM. The second involved all the system's atoms (both QM and MM) calculated at the ONIOM(QM:UFF) level of calculation.[46,47] In both procedures, the reactive part was described by the B3LYP/6-31G* level of calculation and only Cu(I) and the external ligand were optimized while keeping the coordinates of all the rest of the system fixed to their original NMR coordinates. As a result, the di- and tricoordinated species share the same Atox1 original positioning of the conserved cysteine (and when relevant also lysine) residues, and only the position of Cu(I) and the external ligand, which was questionable, differs. We note here that, for the dicoordinated structures, the initial 12 Å distance between Cu(I) and the external ligand was fixed during the optimization. The optimized structures were found to be virtually identical by

dx.doi.org/10.1021/jp210678n | J. Phys. Chem. B 2012, 116, 4425−4432

the two different procedures suggesting that either of them can be used for further calculations (see Table S5 in Supporting Information).

Classical Calculations. To sample protein configurations, the coordinates of the initially optimized reactive part (Cu(I) and the three cysteine-like molecules with the addition of a lysine side chain in some cases) were kept fixed while the rest of the system was subjected to relaxation using molecular dynamics (MD) simulations. All relaxations were performed with the ENZYMIX module of the MOLARIS simulation package.[48,49] Spherical simulation systems of 24 Å radius were divided into four regions. Region I included the reacting fragments (i.e., Cu(I) and the three Cys-like residues with the addition of a Lys side chain in some cases). Region II included the remaining parts of the substrate and protein plus explicit water molecules in and around the protein up to a radius of 22 Å (this part involved more than 1000 water molecules). Region III included protein atoms and water molecules up to a radius of 24 Å that were subjected to distance and polarization constraints according to the surface-constrained all-atom solvent (SCAAS) boundary condition.[48] The rest of the system was represented by a bulk dielectric with a dielectric constant of 80. Long-range electrostatic effects were treated by the local reaction field (LRF) method.[50]

The calculations utilized the ENZYMIX force field for the protein environment.[48,49] A detailed description of the force-field parameters for the reacting fragments and in particular Cu(I) at the various coordination states which were missing in the original ENZYMIX force field and were therefore added, including the respective partial charges, are given in Table S6 and Schemes S1 and S3 in Supporting Information.

The relaxation procedure involved propagation of the whole system during 20 ps of MD, at a temperature of 100 K and with harmonic restraints of 15 kcal mol^{-1} $Å^{-2}$ on the position of all protein heavy atoms, using the respective NMR model structure as the reference structure. The temperature of the system was then gradually raised from 100 K to 298 K, and the harmonic restraints on the protein atoms were gradually released to a value of 0.03 kcal mol^{-1} $Å^{-2}$ during a further 120 ps of simulation time, reaching equilibrium. This ensured that the overall structures of the protein did not deviate much from the observed solution structures. Throughout the simulations, only Lys60 was ionized, due to its expected importance to the stabilization of the Cu(I) center.[14] The overall charge of the system was, therefore, −1 due to the negatively charged external ligand. No counterions were therefore added.

Averaged Structures. Averaged structures for the structural analysis (depicted in Figure 1) were obtained by first relaxing the various structures following the procedure described above. Geometry configurations were collected every 1 ps from the last 50 ps of the relaxation. The resulting structures were obtained each time by averaging over the 50 different configurations that were collected. Figures 1a, 1b and 1c involve an average structure which is based on the solution structure of Atox1 (model 1TL4.2),[14] the crystal structure of Atx1,[25] and the solution structure of Atx1,[21] respectively. Hg(II) in the crystal structure of Atx1 was replaced by Cu(I) in the simulations.

LRA Studies. Our evaluation of the solvation free energy of the external ligand, the copper, or their combined interaction with the environment in the various states (i.e., $\Delta G_{a\rightarrow b}$ and $\Delta G_{e\rightarrow d}$, $\Delta G_{b\rightarrow c}$ and $\Delta G_{f\rightarrow e}$, and $\Delta G_{a\rightarrow c}$ and $\Delta G_{f\rightarrow d}$, respectively, in Scheme 1) is based on the linear response approximation (LRA).[51−53] This approach enables one to estimate the free energy difference between two potential energy surfaces U_1 and U_2 by the following equation:

$$\Delta G_{1\rightarrow 2} = \frac{1}{2}[\langle U_2 - U_1\rangle_1 + \langle U_2 - U_1\rangle_2] \quad (5)$$

where $\langle\rangle_i$ designates an average over trajectories propagated on U_i. The two potential energy surfaces, U_1 and U_2, of the first step in the multiple-step thermodynamic cycle (step a→b in Scheme 1), for example, represent the energy of the whole system (reacting fragments and their environment) when the partial charges of all atoms of the external ligand are considered, U_1, and when they are all set to zero, U_2 (depicted e.g., by states Φ_1 and Φ_2 respectively, in Scheme S1 of Supporting Information). Implementation of eq 5 results, therefore, in the solvation free energy of the external ligand which, in turn, is its interaction with the environment (protein and solvent).

For each combination of coordination and charge distribution of the reactive fragments (states Φ_1, Φ_2, Φ_3, Φ_3', Φ_4, and Φ_5, in Scheme S1 of Supporting Information, describing states, a, b, c, f, e and d, respectively, in Scheme 1), relaxation was first carried out, following the relaxation procedure described above. It is noted that such states are easily defined by the MOLARIS package, using the EVB methodology which describes these states using solely molecular mechanics. Once relaxed, each state was simulated for 50 ps in the protein. All simulations were carried out at 298 K. Geometry configurations were collected every 1 ps, and their respective energy was calculated at the electrostatic embedding level of calculation. Each term of the LRA calculations thus involved averaging over 50 different structural configurations.

The energy calculations at this point involved single-point calculations on each configuration separately at the electrostatic embedding level. That is, the quantum part of the system which involves all the reactive fragments (copper and the three cysteine-like molecules along with the Lys side chain in some cases) was calculated at the PBE0/m6-31+G* level with ZPVE, BSSE, and VdW corrections as described above, while the protein and water molecules were considered as external point charges in the quantum Hamiltonian.[54,55] Different from molecular mechanics calculations, in quantum calculations one cannot set the partial charges of part of the system, e.g., a certain fragment, to zero, as is required for example to describe the hypothetical state b where the partial charges of the external ligand's atoms are all zero (see for example Φ_2 in Scheme S1 of Supporting Information). Thus, the energy of such states was evaluated by calculating the system's energy in the absence of that particular fragment. Namely, the energy of state b for example was obtained from a calculation that did not involve the external ligand.

RESULTS AND DISCUSSION

Validity of the Method for Aliphatic Thiolato Ligands.

Our goal is to establish a suitable level of calculation for reliably predicting the coordination number of Cu(I) in the protein where it is bound to two cysteines and possibly an additional ligand. In an earlier study, we examined the performance of various levels and found that the PBE0/m6-31+G* combined with ZPVE, BSSE, and VdW corrections is suitable when aromatic thiolato ligands are concerned.[30] Therefore, our first step in this work is to validate the predictive power of this level for aliphatic thiolato ligands, which are expected to be better models for cysteines. Recently, Tshuva and co-workers have used two different aliphatic compounds, isopropylthiolate and

dx.doi.org/10.1021/jp210678n | J. Phys. Chem. B 2012, 116, 4425−4432

tert-butylthiolate to prepare Cu(I) complexes. Isopropylthiolato ligand leads mainly to a multinuclear copper cluster where all Cu(I) centers are three coordinated, whereas *tert*-butylthiolato ligand leads to a mononuclear two-coordinate Cu(I) complex.[31] We therefore studied the preferred coordination of these two ligands. In addition, we examined both cysteines and ethylthiolate (our model for cysteine) as ligands.

Table 1 presents ΔE_0 values, including ZPVE, counterpoise corrections,[40] and dispersion corrections,[41,42] for the formation of the tricoordinated complex (eq 2) with the various ligands. The values are given in vacuum, THF, and aqueous solution. The values in THF, which is the crystallization solvent, are in good agreement with the experiment. That is, the large positive value for *tert*-butylthiolate agrees well with the dicoordinated Cu(I) complex observed. The value for isopropylthiolate is very close to zero, indicating, following our earlier experience,[30] a preference for coordination number of three, again, in agreement with the experimental data. These experiments, as well as the various calculated results, are in line with the statement that bulkier ligands demonstrate a larger preference for coordination of two.[30] The bulky *tert*-butylthiol ligand favors the dicoordinated environment, while the other three ligands which are all less hindered demonstrate a smaller preference toward coordination of two and even preference toward tricoordination.

Table 1. ΔE_0 Values (kcal/mol) for the Association Reaction Described in Eq 2 with Various Aliphatic Thiolato Ligands[a,b]

ligand	vacuum	THF	water[c]
$[(CH_3)_3CS]^-$	48.5	6.2	−6.4
$[(CH_3)_2CHS]^-$	46.0	0.3	−8.1
[cysteine]$^-$ [d]	37.5	−0.9	−9.7
$[CH_3CH_2S]^-$	50.7	1.9	−6.9

[a]Energies are given at the PBE0/m6-31+G*//B3LYP/6-31G* level of calculation with solvent corrections by means of PCM, ZPVE, counterpoise corrections and dispersion corrections following our previous studies.[30] [b]Energies in vacuum involved single point calculation on the THF-optimized structures and excluded ZPVE, counterpoise corrections, and dispersion corrections to the energy. [c]For consistency with the gas-phase reaction energies, the values in aqueous solution are given as decimal numbers although the precision of the calculation is expected to be lower, because of the model used (an error on the order of maybe even a few kcal/mol). [d]Cysteine was calculated as $NH_2CH(CH_2S)^-C(=O)OH$.

We are interested in the coordination number of Cu(I) within the protein in the cellular medium. We therefore calculated the coordination in aqueous solution. We can see that water dramatically increased the preference for tricoordination for all the different ligands. We do not have experiments to validate our results in this case, yet this observed trend is expected. Our compounds are all charged, and solvation of the compounds, therefore, plays an important role. That is, the solvation of tricoordinated Cu(I) complexes having an overall charge of (−2) is expected to be higher than the combined solvation of dicoordinated Cu(I) complex and a separate thiolate ligand, having an overall charge of (−1) each. The higher the polarization of the solvent is, the more pronounced this differential solvation would be. Therefore, water (dielectric constant, ε, of 78.39) stabilizes the tricoordinated species more than THF (ε = 7.58) which is less polar and the preference for tricoordination thus increases.

Our conclusion, therefore, is that at this level of calculation, in aqueous solution, results tend to favor and maybe even slightly overestimate tricoordination (as the differences between the different solvents seem somewhat exaggerated). Furthermore, these results emphasize the importance of including the protein environment in the calculations. Any protein and, in particular, copper chaperones are structured species of nonhomogeneous medium and cannot therefore be simply described by a dielectric constant. Thus, prediction of the favored coordination number should involve calculations that account for all the protein atoms explicitly.

Validity of the Thermodynamic Cycles. The whole protein cannot be calculated at the quantum level that was suggested in the previous section. Thus, in practice only the reactive fragments (copper and the three cysteine-like molecules as well as the side chain of Lys60 when included in the QM) were calculated at the PBE0/m6-31+G* level of calculation whereas the environment was accounted for by the electrostatic embedding scheme. That is, all the remaining protein atoms and water molecules were considered as external point charges which were included in the quantum Hamiltonian.[54,55] Furthermore, as mentioned in Methodology, calculation of the reaction energy as suggested by eq 2 is unsuitable within the protein environment. We therefore utilized the LRA approach, which was applied to obtain the reaction free energy following two different thermodynamic cycles (Scheme 1).

Therefore, our next step in this work is to validate this approach. This was done by calculating the reaction free energy for the association of an external thiolato ligand to a dicoordinated Cu(I) in the protein using the sixth model of the solution structure (structure 1TL4.6).[14] The results are presented in the second row of Table 2. The second and third columns in the table list ΔG_0 values obtained from the multi- and two-step cycles, respectively. Both the two- and multistep cycles resulted in a positive reaction free energy, suggesting a preference for dicoordinated copper in agreement with the experimental data. For the two-step cycles, there are in fact two ΔG_0 values resulting from different initial geometries due to different optimization levels (see Computational Details for further information). The similar values 5.5 and 6.2 kcal/mol

Table 2. ΔG_0 Values (kcal/mol) for the Association Reaction in the Protein As Described in Scheme 1 and ΔE_0 Values of the Reactive Fragments Only in Solution Using Eq 2[a]

solution structure	ΔG_0^{MSC}[b]	ΔG_0^{TSC}[b]	ΔG_0^{TSC}[b] with Lys[c]	ΔE_0[d]	ΔE_0[d] with Lys[c]
1TL4.2[e]		5.1	6.0	0.0	−3.9
1TL4.6	3.7[f,g]	5.5;[f] (6.2)[e]	7.7[f]	0.3;[f] (−1.3)[e]	−5.8[f]
1TL4.18[f]		3.6	1.7	0.6	−1.4

[a]For consistency with ΔE_0, we chose to present ΔG_0 values using decimal numbers, although the error for ΔG_0 is found to be ∼3 kcal/mol. [b]ΔG_0^{MSC} and ΔG_0^{TSC} present ΔG_0 obtained from the multiple- and two-step cycles, respectively. [c]ZPVE in this case was calculated at the B3LYP/6-31G* PCM level. [d]Only the reactive fragments calculated at the PBE0/m6-31+G* with solvent effects by means of PCM on geometries optimized as specified. [e]Initial geometry obtained at the B3LYP/6-31G* optimization level in aqueous solution described by the PCM approach. [f]Initial geometry obtained at the ONIOM-(B3LYP/6-31G*:UFF) optimization level. [g]Obtained from only 34 configurations in one of the steps due to convergence difficulties.

dx.doi.org/10.1021/jp210678n | J. Phys. Chem. B 2012, 116, 4425−4432

suggest that the computational method is stable, considering that the results are based on differences between very large quantities. Furthermore, considering the approximations used to calculate the reaction free energy, the two-step and multiple-step cycles are quite comparable (demonstrating ΔG_0 values of 3.7 and 5.5 kcal/mol for the multi- and two-step cycles, respectively). The similar ΔG_0 values suggest that each cycle separately, is appropriate for studying the coordination number with an error of ~3 kcal/mol. Because the two-step thermodynamic cycle involves considerably less computational effort, it was chosen for further studies.

Validity of the Computational Method for Coordination Number Prediction. The reaction free energy for the association of an external ligand to a dicoordinated Cu(I) within the protein was calculated for two additional structures (models 1TL4.2 and 1TL4.18 in the solution structure ensemble). The results are presented in Table 2. The various models, all exhibit positive reaction free energies, ΔG_0, indicating a preference for dicoordinated Cu(I) within the protein, in agreement with the experimental observations,[14,15] as well as other theoretical studies.[20,27,28] Furthermore, the values are all comparable, differing by 3 kcal/mol at most. This result further strengthens the validity of the proposed computational method for prediction.

It is interesting to note that these ΔG_0 values are relatively small, indicating, in turn, that at least thermodynamically no major effort is required to exchange between the two coordination schemes within Atox1. This result, demonstrating energetic feasibility, supports the proposal that Cu(I) transfer involves ligand-exchange reactions including di- and tricoordinated complexes.[18−20]

The conserved Lys (Lys60) is proposed to stabilize the Cu(I) center.[14] Furthermore, it was also suggested to play an essential role in adduct formation with target domains.[60] We therefore recalculated the reaction free energies, using the two-step thermodynamic cycle while including this conserved Lys in the QM region. The ΔG_0 results are presented in the fourth column of Table 2. The table shows that inclusion of Lys does not considerably change the results, exhibiting changes which are within the 3 kcal/mol error of the method. Still, it is interesting to note that the preference for dicoordination usually increases (see results for 1TL4.2 and 1TL4.6 in the first and second entries, respectively). Model 1TL4.18 exhibits a somewhat smaller preference for dicoordination. In view of the respective structures, these trends may be partially explained by the distance of Lys from the Cu(I) center. In the first two models, Lys points toward the MBD and is expected therefore to play a role in the overall stabilization. In the latter model (model 1TL4.18), on the other hand, this Lys points away from the MBD and is therefore expected to play a smaller or different role.

The table also presents reaction energies, ΔE_0, calculated for the various structures in aqueous solution. The values are all virtually zero when Lys60 is not included, suggesting no preference or a small preference for tricoordination.[30] When Lys60 is included, all the values become negative, suggesting that Lys60 itself increases the preference for tricoordination. This result alone is reasonable, because the positively charged Lys60 is expected to stabilize more the higher the overall negative charge of the complex is. Thus, because the tricoordinated Cu(I) complex has a negative charge which is higher than that of the dicoordinated Cu(I) complex (an overall charge of −2 compared to −1 respectively), its better stabilization by Lys60 is clear. The difference between the reaction free energies, ΔG_0, and the reaction energies, ΔE_0, in each entry accounts for the effect of the protein. Therefore, the protein lowers the preference for tricoordination by stabilizing the dicoordinated form.

Possible Rationale for the Dicoordination in Atox1. Two key questions arise: how does Atox1 protein stabilize this special coordination of two, and how does it differ from its homologue copper chaperones that involve tricoordination, e.g., Atx1? Here, we address these questions. The protein stabilizes this special dicoordination of copper using two distinct, yet combined, strategies: structural restraints and stabilizing environment.

Earlier studies suggested that the different coordination in Atxo1 (dicoordination) and its yeast homologue Atx1

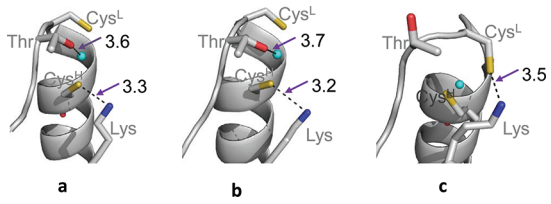

Figure 1. Averaged structures of (a) dicoordinated Cu(I) within Atox1, (b) dicoordinated Cu(I) within Atx1, and (c) tricoordinated Cu(I) within Atx1. Various heavy atom distances reflecting key structural differences are given.

(tricoordination) is associated with the longer α_1 helix in Atox1.[14] Figure 1 presents relaxed structures of the MBD of the dicoordinated Cu(I) structure of Atox1 (Figure 1a), dicoordinated Cu(I) of Atx1 (Figure 1b), and tricoordinated Cu(I) of Atx1 (Figure 1c) as averaged structures. It is clear that the two dicoordinated structures, though presenting different copper chaperones, exhibit a very similar MBD setup which is different from that of the tricoordinated structure. As evident from Figure 1, in both proteins one of the conserved cysteines (referred to as Cys^H hereafter) is part of the helix and its movement is therefore limited, while the other cysteine (referred to as Cys^L hereafter) is part of the loop and is therefore relatively free to move. However, the longer helix in the dicoordinated structures further constrains the relative positioning of the metal-binding cysteines, compared with that of the tricoordinated structure. The two cysteines in the dicoordinated structure are therefore more rigid, keeping an actual S−Cu−S angle which facilitates dicoordination.

Moreover, the relative orientation of the conserved residues changes because of changes in the length of the loop. Significant differences are observed mainly in the behavior of Thr and Lys, resulting in different stabilization schemes of the coordination sphere. In particular, the conserved Lys (Lys60 and Lys65 in Atox1 and Atx1, respectively) is known to have an important role in the stabilization of the MBD.[14,21,28,56,57] In the tricoordinated structures, Lys is relatively close to Cys^L and (though less) to Cys^H, providing electrostatic stabilization for the overall negative charge in the MBD (Figure 1c). In the dicoordinated structures, on the other hand, Lys is close to only one of the Cys residues, Cys^H (Figures 1a,b). Cys^L in these dicoordinated structures may partially benefit from Thr (Thr11 and Thr14 in Atox1 and Atx1, respectively) as suggested in earlier studies.[19,28,58] In addition, this Thr exhibits a relatively short distance from Cu(I), suggesting additional interaction as also pointed out by earlier studies.[25,27,58] We note, in this

dx.doi.org/10.1021/jp210678n | J. Phys. Chem. B 2012, 116, 4425−4432

respect, that in the tricoordinated structure this Thr is oriented away from the MBD, resulting in large distances from both Cys and Cu(I) (for a complete table of distances, see Supporting Information Table S7).

O'Halloran and co-workers proposed a mechanism for Cu(I) transfer which involves the movements of Lys65 in Atx1.[21] Dalosto has also discussed movements of Lys65 to a position which is distant from the binding site upon complex formation.[27] Our calculations further support this proposal, showing that when Lys60 points away from the MBD (third entry in Table 2), the overall preference for dicoordination decreases, facilitating the formation of a transient tricoordinated species. Furthermore, our comparison suggests that movements of lysine in a transfer mechanism may not be unique to Atx1 and can involve additional copper chaperones.[21,57,59,60] Furthermore, in his studies of the interactions within the Atx1-MBD in vacuum, Dalosto also detected a correlated motion between the side chains of both Thr14 and Lys65, which was followed by changes in the S−Cu−S angle.[27] We believe that this correlated motion of lysine and threonine, which is suggested to stabilize a tricoordinated intermediate compound in the transfer mechanism, actually also reduces the stabilization of the dicoordinated Cu(I) and therefore promotes ligation of a third ligand.

Using both structural restraints and environmental stabilization, the protein confines the cysteine residues to a geometry that dictates the special dicoordination. This effect is evident when comparing the ΔE_0 values in Table 2, which were obtained for the reactive fragments within the protein, with ΔE_0 values obtained for the fully optimized model (Table 1, fourth entry). The preference for tricoordination, which is clear in the fully optimized structure (ΔE_0 of −6.9 kcal/mol), decreases considerably within the protein (ΔE_0 ca. 0.0 kcal/mol). This decrease suggests that the geometry of the cysteines within the protein structure is not optimal but rather is dictated by the protein restraints. It also appears that the geometry imposed by the protein involves a lower preference for tricoordination, which in other words can be considered as a higher preference for dicoordination.

CONCLUDING REMARKS

We have demonstrated that the PBE0/m6-31+G* level of calculation, previously shown to properly predict the coordination number of small Cu(I) complexes with aromatic thiolato ligands, is useful for prediction of the preferred coordination in small Cu(I) complexes with aliphatic thiolato ligands as well. We then established a method to predict the preferred Cu(I) coordination in copper chaperones, by combining the PBE0/m6-31+G* quantum level with molecular mechanics and thermodynamic cycles. Calculations demonstrated that addition of a third-external thiolato ligand is unfavorable within the Atox1 protein environment, in agreement with the experimental observations. This validated the ability of the computational approach utilized to properly predict the coordination number of Cu(I) within proteins. Furthermore, analysis of the results and comparison with additional structures led to the conclusion that there is a unique orientation of the active site residues in order to stabilize the dicoordinated Cu(I), which is different from that of the tricoordinated Cu(I) structure. It is shown that the protein applies structural restraints as well as environment stabilization in order to keep this unique Cu(I) dicoordination.

The computational procedure established here to predict the preferred coordination of Cu(I) is not unique to Atox1 and can easily be used for other Cu(I)-containing systems. Successful predictions of Cu(I) coordination in various chaperones and their respective complexes with target proteins may provide additional insights on the transfer mechanism.

ASSOCIATED CONTENT

Supporting Information

Optimized coordinates of the different thiolato Cu(I) complexes that were used to calculated the energies in Table 1 (Tables S1−S4). The tri- and dicoordinated Cu(I) complexes are presented along with the sole thiolato ligand. Coordinates of the reactive part within the sixth model of the 1TL4 solution structure, optimized at the B3LYP/6-31G* PCM level vs the ONIOM(B3LYP/6-31G*:UFF) level (Table S5). Force field parameters which were added to the exsisting ones within ENZYMIX (Table S6), partial charges of di- and tricoordinated Cu(I) at three different charging states according to Scheme 1 as defined with these states (Schemes S1, S2), partial charges of Lys60 when included within the QM calculations (S3) and average distances (Å) within di- and tricoordinated structures of Atox1 and Atx1(Table S7). This material is available free of charge via the Internet at http://pubs.acs.org.

AUTHOR INFORMATION

Corresponding Author

*E-mail: avital@md.huji.ac.il; phone: +972-2-675-8696; fax: +972-2-675-7076.

Notes

The authors declare no competing financial interest.

‡Affiliated with the David R. Bloom Center for Pharmacy at the Hebrew University.

ACKNOWLEDGMENTS

We thank the Human Frontier Science Program (Young investigator grant (RGY)0068-2006) and the Alex Grass Center for Drug Design for financial support.

REFERENCES

(1) Sawyer, D. T.; Sobkowiak, A.; Matsushita, T. *Acc. Chem. Res.* **1996**, *29*, 409−416.
(2) Goldstein, S.; Meyerstein, D. *Acc. Chem. Res.* **1999**, *32*, 547−550.
(3) Rosenzweig, A. C. *Acc. Chem. Res.* **2001**, *34*, 119−128.
(4) Luk, E.; Jensen, L. T.; Culotta, V. C. *J. Biol. Inorg. Chem.* **2003**, *8*, 803−809.
(5) Adlard, P. A.; Bush, A. I. *J. Alzheimer's Dis.* **2006**, *10*, 145−163.
(6) Strozyk, D.; Launer, L. J.; Adlard, P. A.; Cherny, R. A.; Tsatsanis, A.; Volitakis, I.; Blennow, K.; Petrovitch, H.; White, L. R.; Bush, A. I. *Neurobiol. Aging* **2009**, *30*, 1069−1077.
(7) Trumbull, K. A.; Beckman, J. S. *Antioxid. Redox Signaling* **2009**, *11*, 1627−1640.
(8) Madsen, E.; Gitlin, J. D. Copper and iron disorders of the brain. *Annu. Rev. Neurosci.* **2007**, *30*, 317−337.
(9) Bharathi; Indi, S. S.; Rao, K. S. J. *Neurosci. Let.* **2007**, *424*, 78−82.
(10) Vulpe, C.; Levinson, B.; Whitney, S.; Packman, S.; Gitschier, J. *Nat. Genet.* **1993**, *3*, 273−273.
(11) Bull, P. C.; Thomas, G. R.; Rommens, J. M.; Forbes, J. R.; Cox, D. W. *Nat. Genet.* **1993**, *5*, 327−337.
(12) Wernimont, A. K.; Huffman, D. L.; Lamb, A. L.; O'Halloran, T. V.; Rosenzweig, A. C. *Nat. Struct. Biol.* **2000**, *7*, 766−771.
(13) Boal, A. K.; Rosenzweig, A. C. *Chem. Rev.* **2009**, *109*, 4760−4779.

(14) Anastassopoulou, I.; Banci, L.; Bertini, I.; Cantini, F.; Katsari, E.; Rosato, A. *Biochemistry* **2004**, *43*, 13046−13053.
(15) Ralle, M.; Lutsenko, S.; Blackburn, N. J. *J. Biol. Chem.* **2003**, *278*, 23163−23170.
(16) Banci, L.; Bertini, I.; Calderone, V.; Della-Malva, N.; Felli, I. C.; Neri, S.; Pavelkova, A.; Rosato, A. *Biochem. J.* **2009**, *422*, 37−42.
(17) Banci, L.; Bertini, I.; Cantini, F.; Massagni, C.; Migliardi, M.; Rosato, A. *J. Biol. Chem.* **2009**, *284*, 9354−9360.
(18) Banci, L.; Bertini, I.; Cantini, F.; Felli, I. C.; Gonnelli, L.; Hadjiliadis, N.; Pierattelli, R.; Rosato, A.; Voulgaris, P. *Nat. Chem. Biol.* **2006**, *2*, 367−368.
(19) Rodriguez-Granillo, A.; Crespo, A.; Estrin, D. A.; Wittung-Stafshede, P. *J. Phys. Chem. B* **2010**, *114*, 3698−3706.
(20) Holt, B. T. O.; Merz, K. M. *Biochemistry* **2007**, *46*, 8816−8826.
(21) Arnesano, F.; Banci, L.; Bertini, I.; Huffman, D. L.; O'Halloran, T. V. *Biochemistry* **2001**, *40*, 1528−1539.
(22) Banci, L.; Bertini, I.; Del Conte, R.; Markey, J.; Ruiz-Duenas, F. J. *Biochemistry* **2001**, *40*, 15660−15668.
(23) Banci, L.; Bertini, I.; Del Conte, R.; Mangani, S.; Meyer-Klaucke, W. *Biochemistry* **2003**, *42*, 2467−2474.
(24) Pufahl, R. A.; Singer, C. P.; Peariso, K. L.; Lin, S. J.; Schmidt, P. J.; Fahrni, C. J.; Culotta, V. C.; PennerHahn, J. E.; Ohalloran, T. V. *Science* **1997**, *278*, 853−856.
(25) Rosenzweig, A. C.; Huffman, D. L.; Hou, M. Y.; Wernimont, A. K.; Pufahl, R. A.; O'Halloran, T. V. *Structure* **1999**, *7*, 605−617.
(26) Hearnshaw, S.; West, C.; Singleton, C.; Zhou, L.; Kihlken, M. A.; Strange, R. W.; Le Brun, N. E.; Hemmings, A. M. *Biochemistry* **2009**, *48*, 9324−9326.
(27) Dalosto, S. D. *J. Phys. Chem. B* **2007**, *111*, 2932−2940.
(28) Rodriguez-Granillo, A.; Wittung-Stafshede, P. *J. Phys. Chem. B* **2008**, *112*, 4583−4593.
(29) Banci, L.; Bertini, I.; Ciofi-Baffoni, S.; Kozyreva, T.; Zovo, K.; Palumaa, P. *Nature* **2010**, *465*, 645−648.
(30) Ansbacher, T.; Srivastava, H. K.; Martin, J. M. L.; Shurki, A. *J. Comput. Chem.* **2010**, *31*, 75−83.
(31) Kohner-Kerten, A.; Tshuva, E. Y. *J. Organomet. Chem.* **2008**, *693*, 2065−2068.
(32) Goj, L. A.; Blue, E. D.; Delp, S. A.; Gunnoe, T. B.; Cundari, T. R.; Pierpont, A. W.; Petersen, J. L.; Boyle, P. D. *Inorg. Chem.* **2006**, *45*, 9032−9045.
(33) Hoyau, S.; Ohanessian, G. *J. Am. Chem. Soc.* **1997**, *119*, 2016−2024.
(34) Rosen, B. M.; Percec, V. *J. Polym. Sci., Polym. Chem.* **2007**, *45*, 4950−4964.
(35) Miertus, S.; Scrocco, E.; Tomasi, J. *Chem. Phys.* **1981**, *55*, 117−129.
(36) Perdew, J. P.; Burke, K.; Ernzerhof, M. *Phys. Rev. Lett.* **1996**, *77*, 3865−3868.
(37) Adamo, C.; Barone, V. *J. Chem. Phys.* **1999**, *110*, 6158−6170.
(38) Mitin, A. V.; Baker, J.; Pulay, P. *J. Chem. Phys.* **2003**, *118*, 7775−7782.
(39) Rassolov, V. A.; Ratner, M. A.; Pople, J. A.; Redfern, P. C.; Curtiss, L. A. *J. Comput. Chem.* **2001**, *22*, 976−984.
(40) Boys, S. F.; Bernardi, F. *Mol. Phys.* **1970**, *19*, 553−566.
(41) Grimme, S. *J. Comput. Chem.* **2004**, *25*, 1463−1473.
(42) Grimme, S. *J. Comput. Chem.* **2006**, *27*, 1787−1799.
(43) Karton, A.; Tarnopolsky, A.; Lamere, J. F.; Schatz, G. C.; Martin, J. M. L. *J. Phys. Chem. A* **2008**, *112*, 12868−12886.
(44) Frisch, M. J.; Trucks, G. W.; Schlegel, H. B.; Scuseria, G. E.; Robb, M. A.; Cheeseman, J. R.; Scalmani, G.; Barone, V.; Mennucci, B.; Petersson, G. A., et al. *Gaussian 09, Revision A.1*; Gaussian, Inc., Wallingford, CT, 2009.
(45) Kerdcharoen, T.; Birkenheuer, U.; Kruger, S.; Woiterski, A.; Rosch, N. *Theor. Chem. Acc.* **2003**, *109*, 285−297.
(46) Dapprich, S.; Komaromi, I.; Byun, K. S.; Morokuma, K.; Frisch, M. J. *J. Mol. Struct.: THEOCHEM* **1999**, *461*, 1−21.
(47) Rappe, A. K.; Casewit, C. J.; Colwell, K. S.; Goddard, W. A.; Skiff, W. M. *J. Am. Chem. Soc.* **1992**, *114*, 10024−10035.
(48) King, G.; Warshel, A. *J. Chem. Phys.* **1989**, *91*, 3647−3661.
(49) Chu, Z.; Villa, J.; Strajbl, M.; Schutz, C.; Shurki, A.; Warshel, A. *MOLARIS version beta 9.05*; University of Southern California, Los Angeles, 2004.
(50) Lee, F. S.; Warshel, A. *J. Chem. Phys.* **1992**, *97*, 3100−3107.
(51) Sham, Y. Y.; Chu, Z. T.; Tao, H.; Warshel, A. *Proteins* **2000**, *39*, 393−407.
(52) Lee, F. S.; Chu, Z. T.; Bolger, M. B.; Warshel, A. *Protein Eng.* **1992**, *5*, 215−228.
(53) Kubo, R.; Toda, M.; Hashitsume, N. *Statistical Physics II: Nonequilibrium Statistical Mechanics*; Springer-Verlag: Berlin, 1985.
(54) Hall, G. G.; Smith, C. M. *Int. J. Quantum Chem.* **1984**, *25*, 881−890.
(55) Smith, C. M.; Hall, G. G. *Theor. Chim. Acta* **1986**, *69*, 63−69.
(56) Banci, L.; Bertini, I.; Cantini, F.; Ciofi-Baffoni, S. *Cell. Mol. Life Sci.* **2010**, *67*, 2563−2589.
(57) Arnesano, F.; Banci, L.; Bertini, I.; Ciofi-Baffoni, S.; Molteni, E.; Huffman, D. L.; O'Halloran, T. V. *Gen. Res.* **2002**, *12*, 255−271.
(58) Rodriguez-Granillo, A.; Wittung-Stafshede, P. *Biochemistry* **2009**, *48*, 960−972.
(59) Portnoy, M. E.; Rosenzweig, A. C.; Rae, T.; Huffman, D. L.; O'Halloran, T. V.; Culotta, V. C. *J. Biol. Chem.* **1999**, *274*, 15041−15045.
(60) Hussain, F.; Rodriguez-Granillo, A.; Wittung-Stafshede, P. *J. Am. Chem. Soc.* **2009**, *131*, 16371−16373.